11th International Symposium on Turbulence and Shear Flow Phenomena (TSFP11)
Southampton, UK, July 30 to August 2, 2019

ANALYSIS OF THE VERTICAL SPECTRA OF DENSITY FLUCTUATION VARIANCE IN THE STRONGLY STRATIFIED TURBULENCE.

Victor Avsarkisov
Department Theory and Modelling
Leibniz Institute of Atmospheric Physics
18225 Kühlungsborn, Germany
avsarkisov@iap-kborn.de

Boris Strelnikov
Department Optical Soundings & Sounding Rockets
Leibniz Institute of Atmospheric Physics
18225 Kühlungsborn, Germany
strelnikov@iap-kborn.de

Erich Becker
Department Theory and Modelling
Leibniz Institute of Atmospheric Physics
18225 Kühlungsborn, Germany
becker@iap-kborn.de

ABSTRACT

We utilized measurements obtained during WADIS-2 sounding rocket campaign to study the strongly stratified turbulence that is present in the mesosphere and lower thermosphere region. The measurements are complemented by results from the global circulation model that suggest that the gravity wave breaking generates a strongly stratified turbulent regime in mesosphere. It is found that at very high buoyancy Reynolds numbers, such as $Re_b = 1000$, and sufficiently low horizontal Froude numbers, such as $Fr_h < 0.01$ vertical spectra of density fluctuation variance exhibits k_z^{-1} spectral range in the region between buoyancy (k_z^{-3}) and inertial ($k_z^{-5/3}$) subranges.

INTRODUCTION

It is well known, that winter mesosphere is the home of a very energetic process, which is responsible for an energy injection into mesoscales and generation of a turbulence (Fritts & Alexander, 2003; Becker & Vadas, 2018). This process is a gravity wave breaking and it takes place in the mesosphere and lower thermosphere (MLT) region between 50 and 100 km at the middle and high latitudes. The energy released from the breaking process transforms into stratified turbulence (Billant & Chomaz, 2001; Lindborg, 2006) which can be observed remotely by radars or lidars and precisely measured in-situ by sounding rockets.

ROCKET MEASUREMENTS

In this work we utilize measurements obtained during the WADIS-2 sounding rocket campaign, which is a part of WADIS project. WADIS stands for WAve propagation and DISsipation in the middle atmosphere. A detailed description of WADIS mission, particular rocket campaign, and overview of measured parameters can be found in Strelnikov *et al.* (2017) and Strelnikov *et al.* (2019). The WADIS rocket experiment was configured to earn the best quality turbulence measurements available to date in the altitude range from 60 to 110 km. The rocket was launched from north Norwegian Andøya Space Center (ASC, 69°N, 16°E) on 5 of March 2015 at 01:44 UTC. The ASC is located close to the ALOMAR observatory (von Zahn & Rees, 1994) and, therefore, a vast of ground based observations complemented the rocket-borne measurements yielding, among other things horizontal wind measurements (see Strelnikov *et al.*, 2019, for more details).

The applied turbulence measurement technique is based on the fact that turbulence creates fluctuations in density of neutral air which is shown to be a conservative and passive turbulence tracer at scales smaller than Ozmidov length scale in the MLT (Lübken, 1992; Lübken *et al.*, 1993; Lübken, 1997). The ionization gauge CONE (COmbined measurements of Neutrals and Electrons) carried by a sounding rocket measures vertical profile of tiny density fluctuations (down to 0.01 %) which are used to derive the turbulence kinetic energy dissipation rate, ε_K. We apply a spectral model method introduced by Lübken (1992) and extended by Strelnikov *et al.* (2003) to derive ε_K-altitude profile with 100 m vertical resolution. A detailed description of this instrument, data analysis technique, measurement uncertainties, and gathered geophysical results can be found in Strelnikov *et al.* (2013). Importantly, apart from density fluctuations measurements for turbulence analysis, CONE yield absolute density and temperature altitude profiles measured in the same measurement volume. Within the altitude region relevant for this study absolute density and temperature measurements error does not exceed 2 % and 2 K, respectively. This allows to precisely derive background parameters like kinematic viscosity ν using Sutherland's formula (e.g. Sissenwine *et al.*, 1962) or Brunt-Väisälä (buoyancy) frequency N.

Briefly, the spectral model analysis technique works as follows. We derive power spectral densities of the turbulent tracer (spatial fluctuations of neutral air density) and fit a theoretical function that covers both the inertial (i.e. the

Table 1. Summary of measurements obtained during the WADIS-2 rocket campaign. Here $Re_b = \varepsilon_K/\nu N^2$; $Fr_h = \varepsilon_K/NU_h^2$; $L_o = \sqrt{\varepsilon_K/N^3}$ and $L_b = U_h/N$, where ε_K is the turbulent kinetic energy dissipation rate, ν is the kinematic viscosity, N is the buoyancy frequency and U_h is the horizontal root-mean-square of the velocity fluctuation.

Case	Re_b	Fr_h	ε_K (m^2/s^3)	L_o (m)	L_b (m)	N $(1/s)$	Altitude range (km)
RE10	10.0	1.6×10^{-4}	$8.7\times10^{-4}\pm21\%$	11.7	1058.4	1.9×10^{-2}	69.3 - 69.6
RE100	102.2	5.9×10^{-4}	$1.3\times10^{-2}\pm41\%$	42.3	1752.5	1.9×10^{-2}	70.7 - 70.9
RE500	501.1	1.2×10^{-3}	$3.7\times10^{-2}\pm29\%$	64.5	1883.2	2.1×10^{-2}	66.8 - 66.9
RE1000	998.4	7.6×10^{-3}	$6.6\times10^{-2}\pm33\%$	81.7	935.4	2.1×10^{-2}	65.4 - 65.5

$k_z^{-5/3}$ slope) and the viscous part (i.e. the steeper part towards higher k_z) of the spectrum. The break in the spectrum is given by ε_K and ν only (ν is the kinematic viscosity derived from simultaneously measured background densities and temperatures) and is used to unambiguously derive ε_K. The length scale where this break occurs is called the inner scale and is related to the Kolmogorov scale (e.g., Lübken, 1992). Typical values of the inner scale measured in MLT are in the range from 10 to 50 m (e.g., Lübken *et al.*, 2002). The instrument is moved through the MLT region with a speed of ∼1000 m/s. The measured data is sampled with frequency of 3.3 kHz which results in a theoretical altitude resolution of approximately 30 cm. The effective, i.e. actual resolution of the measured spectra is rather limited by a noise-floor of the instrument and for strong to weak turbulence is between 1 and 10 m. Note, that the spectral model technique used to derive ε_K does not utilize the absolute value of density fluctuations, i.e. their variance, but only the frequency (or k) dependence of the measured spectra.

The WADIS-2 rocket campaign utilized both the in-situ and ground-based measurement techniques to study the small-scale fluctuations in different quantities, including density, temperature, as well as horizontal mean and root-mean-square velocity fluctuations.

Horizontal wind velocities were measured both by ALOMAR RMR (von Zahn *et al.*, 2000; Baumgarten, 2010) and Na Weber lidars She *et al.* (2002); Arnold & She (2003) to cover altitude range from 20 km to ∼105 km. Limited spatial resolution of the horizontal wind measurements (∼150 m) by the ground-based lidars only allows to characterize the background atmosphere and is not sufficient to derive energy dissipation rate ε_K (see Baumgarten, 2010; Lübken *et al.*, 2016; Strelnikov *et al.*, 2019, for details). Besides this, in order to obtain a reasonable signal-to-noise ratio (SNR), horizontal root-mean-square velocity fluctuation measurements must be averaged over at least 15 min. Another source of uncertainty in velocity fluctuations data for our study is that they were conducted not exactly in the same measurement volume as the rocket soundings. Taking into account absolute horizontal wind speeds of ∼50–100 ms^{-1} at MLT altitudes, it is well justified that these data adequately represent mean state of the background atmosphere during the rocket experiment (see Strelnikov *et al.*, 2019, for experiment and data description in more detail).

VERTICAL SPECTRA OF DENSITY FLUCTUATION VARIANCE

Stratified turbulence generated by the GW breaking process can be found in different states at different altitudes in the winter MLT region. At altitudes above 80 km the stratified shear flow instabilities arise when the Miles-Howard criterion for stability is violated (Miles, 1961; Howard, 1961). This gives rise to the development of Kelvin-Helmholtz instabilities (KHI). However, when stratification is strong and the thickness of the layer of inflectional shear (buoyancy scale L_b) is much larger than the thickness of any passive scalar (outer scale of isotropic turbulence or Ozmidov scale L_o) in the stable density gradient, we can observe bifurcation of the KHI into the Holmboe wave instability (HWI) (Holmboe, 1962; Peltier, 2003). Most energetic regimes of the latter type of turbulence in terms of buoyancy Reynolds number with strong stratification (in terms of horizontal Froude number) have been found in the region between 55 km and 70 km. Examples of this type of stratified turbulence are listed in the Table 1 (cases from RE10 through RE1000). This regime is called strongly stratified turbulence (SST) (Billant & Chomaz, 2001; Lindborg, 2006; Davidson, 2013) or layered anisotropic stratified turbulence (LAST) (Falder *et al.*, 2016; Lucas *et al.*, 2017). The latter name of this regime indicates the presence of the well-mixed layers with sharp density interfaces, which are

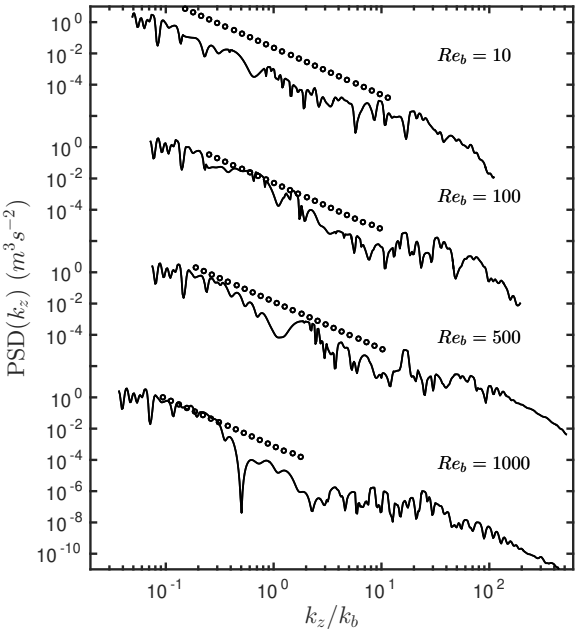

Figure 1. Vertical spectra PSD(k_z) versus k_z/k_b, where $k_b = L_b^{-1}$. Buoyancy Reynolds number grows from $Re_b = 10$ (top) to $Re_b = 1000$ (bottom). Circle straight lines correspond to $N^2 k_z^{-3}$ range of stratified turbulence.

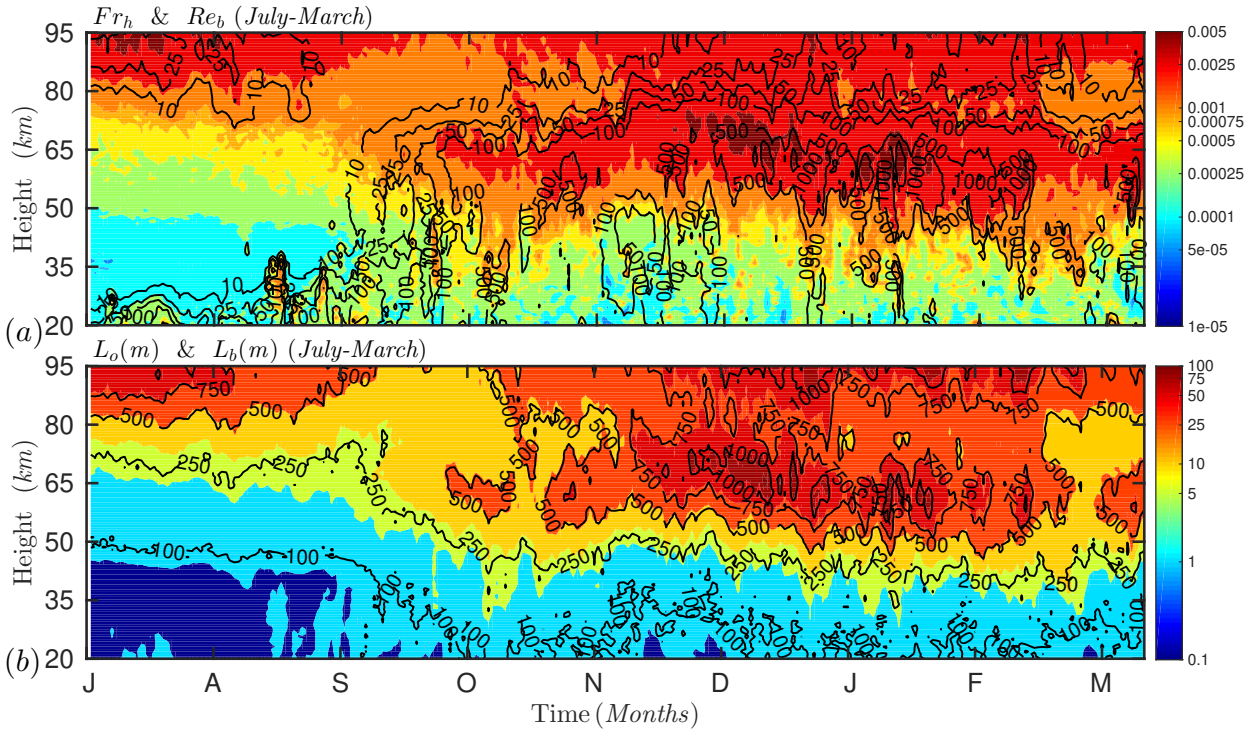

Figure 2. (*a*) Nine months cycle of Fr_h (shown in colors) and Re_b (shown in contours) obtained from KMCM at latitude of ASC (69°N). (*b*) Nine months cycle of $L_o = \sqrt{\varepsilon_K/N^3}$ (shown in colors) and $L_b = U_h/N$ (shown in contours)

also known as the pancake vortices. Routes to the spontaneous layering in strongly stratified regime are still an important subject of investigation and they include gravity wave breaking, intrusions from a density currents and shear flow instabilities (Thorpe, 2016).

Figure 1 shows the power spectral density (PSD) of density fluctuation variance versus vertical wavenumber scaled with k_b, where $k_b = 1/L_b$ and $L_b = U_h/N$ is the buoyancy scale and U_h is the horizontal rms velocity fluctuation. The buoyancy Reynolds number $Re_b = \varepsilon_K/(\nu N^2)$ increases from top to the bottom from ten to one thousand (for more detail, see Table 1).

As it can be seen from figure 1 at low Re_b and horizontal Froude number $Fr_h = \varepsilon_K/(NU_h^2)$ we see a k_z^{-3} region that spans almost for two decades. This region is characterized by gravity waves and turbulent pancake structures and is called stratified buoyancy spectrum range. As the Re_b and Fr_h increase to $Re_b = 100$ and $Fr_h = 5.9 \times 10^{-4}$, respectively, the buoyancy range becomes narrower while inertial range broadens. At larger buoyancy Reynolds numbers ($Re_b = 500$) k_z^{-3} range becomes narrower as Fr_h further increases in size. The narrowest k_z^{-3} range (if such even exist) was found in the RE1000 case, as it shrinks to half decade.

RESULTS FROM THE GENERAL CIRCULATION MODEL (GCM)

Apart from the in-situ sounding rocket measurements in the present analysis we employ a gravity wave resolving GCM. The Kühlungsborn Mechanistic general Circulation Model (KMCM) is a free-running atmospheric GCM which spans from the Earth surface up to the lower thermosphere (135 km) (Becker & Vadas, 2018). The model employs a standard dynamical spectral core in streamwise and spanwise (horizontal) directions and a staggered vertical grid as it was initially proposed by (Simmons & Burridge, 1981). The horizontal grid space resolution is 55 km, while vertical is ∼600 m between the surface and ∼100 km. The model also has an enhanced orography, which allows to avoid parametrization of orographic gravity waves. Modelling of all subgrid-scale processes in the KMCM fulfill the energy conservation law. For unresolved dynamical scales a Smagorinsky's diffusion parametrization scheme is employed for both horizontal and vertical diffusion (Becker & Burkhardt, 2007). In the current version of the model we couple the resolved flow with the sub-grid scale scheme by means of hard interfacing strategy (Fröhlich & von Terzi, 2008), which uses prescribed horizontal and vertical mixing lengths.

In order to check if KMCM provides us with similar stratified turbulence regime as it is presented in Table 1, we simulated certain non-dimensional parameters such as Re_b, Fr_h and length scales L_b and L_o. Results of the numerical simulation are shown on figure 2. As it can be taken from figure 2 (*a*) horizontal Froude number is below critical value of $Fr_h = 0.02$ proposed in Lindborg (2006). KMCM correctly simulates an increase of the Re_b in the region between 55 km and 70 km in winter months. This increase of the stratified turbulence in mesosphere is associated with a very intensive gravity wave breaking process that takes place in the mesosphere in winter months (Avsarkisov *et al.*, 2019; Becker & Vadas, 2018). Both parameters shown on figure 2 (*a*), Fr_h and Re_b that define the strength of the strongly stratified regime, nicely fit to experimental measurements from the WADIS-2 sounding rocket campaign. Figure 2 (*b*) suggests that length scales listed in table 1 are very similar to the length scales simulated with KMCM. Figure 2 (*b*) also indicates that there is a certain correlation between the buoyancy and Ozmidov scales and that with increase of the buoyancy Reynolds number up to $Re_b = 1000$ the ratio L_b/L_o becomes very close to ten.

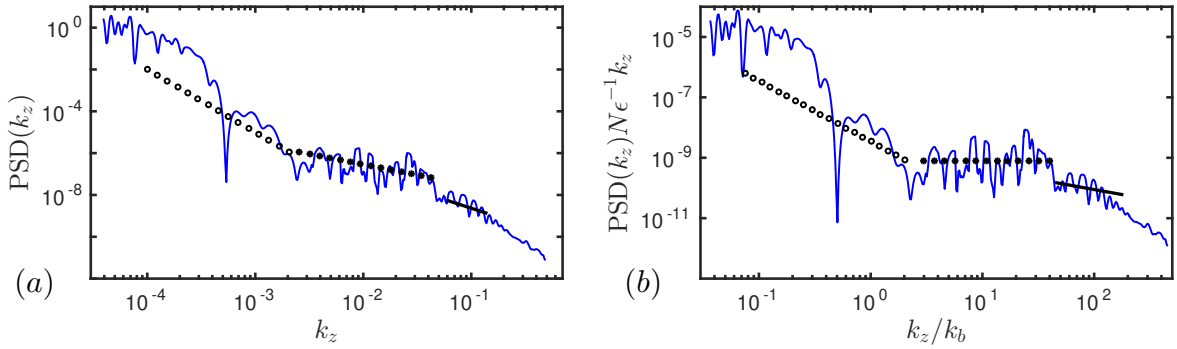

Figure 3. Vertical spectra of density fluctuation variance for RE1000 case. (*a*) Non-compensated form. (*b*) Compensated vertical spectra PSD$(k_z)N\varepsilon_K^{-1}k_z$ versus k_z/k_b, where $k_b = L_b^{-1}$. Circle straight lines correspond to $N^2k_z^{-3}$ range, dotted lines to $N^{-1}\varepsilon_K k_z^{-1}$ range and solid lines to $\varepsilon_K^{-2/3}k_z^{-5/3}$ range.

HIGH-REYNOLDS-NUMBER EFFECTS

Probably the most important property of the high-Reynolds-number wall-bounded turbulence is the scale separation between near-wall and outer regions (Perry *et al.*, 1986; Smits *et al.*, 2011). This scale separation is caused by the presence of a very large scale structures in the outer region of the flow and small-scale isotropic structures in the near-wall region. A similar variety of structures is observed in the strongly stratified turbulence, where there are large pancake-like structures and gravity waves that live in the stratified turbulence and small-scale (Ozmidov scale or smaller) size structures that live in the isotropic turbulence. This similarity between wall-bounded and strongly stratified turbulence allows us to suggest that the similar scale separation should be present in the high-Reynolds-number strongly stratified turbulence.

As it can be seen from figure 1, $Re_b = 100$ is not high enough to detect such a region of the scale separation. However, at $Re_b = 500$ the overlap region is already emerged and it becomes wider with increase of the buoyancy Reynolds number. At $Re_b = 1000$ the region spans almost from the buoyancy to the inertial subrange over one decade in k_z.

An implication to the form of the slope in the overlap region can be made by analysis of vertical spectra (Billant & Chomaz, 2001), which can be defined by $E_K(k_z) \propto U^2/k_z$. Using the assumption that U is a characteristic velocity scale in inertial range $U = U_{L_o} = \sqrt{\varepsilon_K/N}$, it is found that $E_K(k_z)$ should be of the form

$$E_K(k_z) \propto \varepsilon_K N^{-1} k_z^{-1}. \qquad (1)$$

The vertical spectrum of density fluctuation variance at $Re_b = 1000$ in uncompensated and compensated by multiplication by $N\varepsilon_K^{-1}k_z$ forms is shown in figure 3. It provides a clear support for a k_z^{-1} form of the spectrum in the strongly stratified region between the buoyancy and inertial subranges. The overlap region first emerges when $Re_b = 300$ and $Fr_h < 0.01$ (not shown here). As it can be taken from figure 1 the scale separation k_z^{-1} range gets wider as Re_b grows, while both the strongly stratified (k_z^{-3}) and the inertial ($k_z^{-5/3}$) regions become narrower.

CONCLUSIONS

In the present study we analyze a new results from the in-situ sounding rocket measurements in winter MLT region at middle latitudes. It is found, that atmosphere in this region is in the strongly stratified turbulent regime. The measurements performed in the current study are made at very high Re_b numbers, which are by far out of the range of capabilities of present day experiments and simulations. Very low horizontal Froude numbers Fr_h indicate that turbulence should be induced by the Holmboe wave instability. Due to its complexity this turbulence regime is not well studied yet and we believe that our study can fill some gaps in the theory of stratified turbulence. In particular, present measurements and analytic results resolve an open issue of the presence of k_z^{-3} buoyancy spectral range and suggest a new scale separation k_z^{-1} range that emerges at high buoyancy Reynolds numbers, when Fr_h is sufficiently low.

The new k_z^{-1} spectral range is observed in the region between buoyancy and inertial subranges. It should not be mixed with the well known k^{-1} Batchelor spectrum (Batchelor, 1959), as the latter one is observed at scales much smaller than Ozmidov scale. Apart from that, for neutral air density fluctuations in the winter MLT region, e.g., Lübken (1992, 1997) showed, that for scales below the buoyancy scale which, for MLT is of order kilometer the Schmidt number is close to one.

In the present study we propose that the new k_z^{-1} spectral range is a scale separation region that emerges between buoyancy and inertial subranges at high Re_b. This analogy between the wall-bounded turbulence and the strongly stratified turbulence is even clearer in this respect if we recall that both these turbulent flows are strongly affected by the vertical shear of the horizontal velocity.

REFERENCES

Arnold, K. S. & She, C. Y. 2003 Metal fluorescence lidar (light detection and ranging) and the middle atmosphere. *Contemporary Physics* **44**, 35–49.

Avsarkisov, V., Becker, E. & Renkwitz, T. 2019 Turbulent coherent structures in the middle atmosphere: Theoretical estimates deduced from a gravity-wave resolving general circulation model. *In preparation* .

Batchelor, G. K. 1959 Small-scale variation of convected quantities like temperature in turbulent fluid. part 1. general discussion and the case of small conductivity. *J. Fluid Mech.* **5**, 113–133.

Baumgarten, G 2010 Doppler rayleigh/mie/raman lidar for wind and temperature measurements in the middle

atmosphere up to 80 km. *Atmospheric Measurement Techniques* **3** (6), 1509.

Becker, E. & Burkhardt, U. 2007 Nonlinear horizontal diffusion for GCMs. *Mon. Wea. Rev.* **135**, 1439–1454.

Becker, E. & Vadas, S. L. 2018 Secondary gravity waves in the winter mesosphere: Results from a high-resolution global circulation model. *J. Geo. Res.:Atmos.* **123**, 2605–2627.

Billant, P. & Chomaz, J.-M. 2001 Self-similarity of strongly stratified inviscid flows. *Phys. Fluids* **13** (6), 1645–1651.

Davidson, P. A. 2013 *Turbulence in Rotating, Stratified and Electrically Conducting Fluids*. Cambridge University Press.

Falder, M., White, N. J. & Caulfield, C. P. 2016 Seismic imaging of rapid onset of stratified turbulence in the South Atlantic Ocean. *J. Phys. Ocean.* **46**, 1023–1044.

Fritts, D. C. & Alexander, M. J. 2003 Gravity wave dynamics and effects in the middle atmosphere. *Rev. Geophys.* **41** (1 / 1003), 3–1–64.

Fröhlich, J. & von Terzi, D. 2008 Hybrid LES/RANS methods for the simulation of turbulent flows. *Prog. Aero. Sci.* **44**, 349–377.

Holmboe, J. 1962 On the behaviour of symmetric waves in stratified shear layers. *Geofys. Publ. Oslo* **24**, 67–113.

Howard, L. N. 1961 Note on a paper of john w. miles. *J. Fluid Mech.* **10**, 509–512.

Lindborg, E. 2006 The energy cascade in a strongly stratified fluid. *J. Fluid Mech.* **550**, 207–242.

Lübken, F.-J. 1992 On the extraction of turbulent parameters from atmospheric density fluctuations. *J. Geophys. Res.* **97**, 20,385–20,395.

Lübken, F.-J. 1997 Seasonal variation of turbulent energy dissipation rates at high latitudes as determined by insitu measurements of neutral density fluctuations. *J. Geophys. Res.* **102**, 13,441–13,456.

Lübken, F.-J., Baumgarten, G., Hildebrand, J. & Schmidlin, F. J. 2016 Simultaneous and co-located wind measurements in the middle atmosphere by lidar and rocketborne techniques. *Atmospheric Measurement Techniques Discussions* **2016**, 1–23.

Lübken, F.-J., Hillert, W., Lehmacher, G. & von Zahn, U. 1993 Experiments revealing small impact of turbulence on the energy budget of the mesosphere and lower thermosphere. *J. Geophys. Res.* **98**, 20,369–20,384.

Lübken, F.-J., Rapp, M. & Hoffmann, P. 2002 Neutral air turbulence and temperatures in the vicinity of polar mesosphere summer echoes. *J. Geophys. Res.* **107(D15)**, 4273–4277.

Lucas, D., Caulfield, C. P. & Kerswell, R. R. 2017 Layer formation in horizontally forced stratified turbulence: connecting exact coherent structures to linear instabilities. *J. Fluid Mech.* **832**, 409–437.

Miles, J. W. 1961 On the stability of heterogeneous shear flows. *J. Fluid Mech.* **10**, 496–508.

Peltier, W. R. 2003 Mixing efficiency in stratified shear flows. *Annu. Rev. Fluid Mech.* **35**, 135–167.

Perry, A. E., Henbest, S. M. & Chong, M. S. 1986 A theoretical and experimental study of wall turbulence. *J. Fluid Mech.* **119**, 163–199.

She, C. Y., Vance, J. D., Williams, B. P., Krueger, D. A., Moosmuller, H., Gibson-Wilde, D. & Fritts, D. 2002 Lidar studies of atmospheric dynamics near polar mesopause. *EOS Transactions* **83**, 289–.

Simmons, A.J. & Burridge, D.M. 1981 An energy and angular momentum conserving vertical finite-difference scheme and hybrid vertical coordinates. *Mon. Weather Rev.* **109**, 758–766.

Sissenwine, N., Dubin, M. & Wexler, H. 1962 The U. S. Standard Atmosphere. *J. Geophys. Res.* **67**, 3627–3630.

Smits, A. J., McKeon, B. J. & Marusic, I. 2011 High-Reynolds number wall turbulence. *Annu. Rev. Fluid Mech.* **43**, 353–375.

Strelnikov, B., Rapp, M. & Lübken, F. 2013 *In-situ density measurements in the mesosphere/lower thermosphere region with the TOTAL and CONE instruments*, pp. 1–11. Terrapub.

Strelnikov, B., Rapp, M. & Lübken, F.-J. 2003 A new technique for the analysis of neutral air density fluctuations measured in situ in the middle atmosphere. *Geophys. Res. Let.* **30**, 2052.

Strelnikov, B., Staszak, T., Asmus, H., Strelnikova, I., Grygalashvyly, M., Lübken, F.-J., Latteck, R., Baumgarten, G., Höffner, J., Wörl, R., Rapp, M., Fasoulas, S., Löhle, S., Eberhart, M., Williams, B.-P., Friedrich, M., Hedin, J., Khaplanov, M., Gumbel, J. & Barjatya, A. 2019 Simultaneous in situ measurements of small-scale structures in neutral, plasma, and atomic oxygen densities during WADIS sounding rocket project. *Atmos. Chem. and Phys.* p. submitted.

Strelnikov, B., Szewczyk, A., Strelnikova, I., Latteck, R., Baumgarten, G., Lübken, F.-J., Rapp, M., Fasoulas, S., Löhle, S., Eberhart, M., Hoppe, U.-P., Dunker, T., Friedrich, M., Hedin, J., Khaplanov, M., Gumbel, J. & Barjatya, A. 2017 Spatial and temporal variability in MLT turbulence inferred from in situ and ground-based observations during the WADIS-1 sounding rocket campaign. *Annales Geophysicae* **35**, 547–565.

Thorpe, S. A. 2016 Layers and internal waves in uniformly stratified fluids stirred by vertical grids. *J. Fluid Mech.* **793**, 380–413.

von Zahn, U. & Rees, D. 1994 The ALOMAR observatory for middle atmosphere research. *STEP International* **4** (6), 12–14.

von Zahn, U., von Cossart, G., Fiedler, J., Fricke, K. H., Nelke, G., Baumgarten, G., Rees, D., Hauchecorne, A. & Adolfsen, K. 2000 The ALOMAR Rayleigh/Mie/Raman lidar: objectives, configuration, and performance **18**, 815–833.